Hindawi
Advances in Materials Science and Engineering
Volume 2018, Article ID 1249615, 8 pages
https://doi.org/10.1155/2018/1249615

Research Article

Interaction of Magnesia with Limestone-Metakaolin-Calcium Hydroxide Ternary Alkali-Activated Systems

A. Cwirzen,[1] **L. Metsäpelto,**[2,3] **and K. Habermehl-Cwirzen**[4]

[1]*Professor, Luleå University of Technology, SE-97187 Luleå, Sweden*
[2]*MSc, YIT Infra Oy, Salmisaarenaukio 2, 00180 Helsinki, Finland*
[3]*Formerly MSc Student at Aalto University, Espoo, Finland*
[4]*PhD, Senior Lecturer, Luleå University of Technology, SE-97187 Luleå, Sweden*

Correspondence should be addressed to A. Cwirzen; andrzej.cwirzen@ltu.se

Received 23 May 2018; Accepted 14 October 2018; Published 14 November 2018

Academic Editor: Luís Evangelista

The effect of magnesia on ternary systems composed of limestone, metakaolin and calcium hydroxide, alkali activated with sodium silicate, sodium hydroxide, and sodium sulphate was studied by determination of the compressive strength, X-ray powder diffraction (XRD), thermogravimetry (TG), and scanning electron microscope (SEM). Pastes activated with sodium silicate and sodium sulphate showed strength regression caused by a formation of an unstable prone to cracking geopolymer gel. The presence of magnesia in sodium hydroxide-activated system hindered this trend by promoting a formation of more stable crystalline phases intermixed with brucide. In general, magnesia densified the binder matrix by promoting a formation of amorphous phases while sodium hydroxide produced the most porous microstructure containing high amount of crystalline phases.

1. Introduction

It is estimated that the production of one ton of Portland cement clinker causes emission of approximately 800 kilograms of carbon dioxide into the atmosphere. The cement industry alone accounts globally for a staggering 8% share of a total annually manmade carbon dioxide [1]. The cement industry is continuously modernizing the production process and uses more secondary cementitious binders such as fly ash, limestone, or blast-furnace slag to improve the situation. There are also alternative cementitious binders including the so-called geopolymers; Provis et al. [2] and Purdon [3]. At present, these binders are commercially available and used mostly in Europe and Australia [4–6]. Geopolymers can be defined as synthetic aluminosilicates inorganic polymers [7]. The most commonly used aluminosilicate precursors include fly ash (FA), blast-furnace slag (BFS), and metakaolin (MK) [8–10]. Fly ash and blast-furnace slag are industrial by-products with limited availability and increasing price. Metakaolin on the other hand is produced from natural kaolin clays through energy consuming and CO_2 emitting calcination process [11, 12]. Alkali-activated slag upon dissolution forms mainly calcium silicate hydrate incorporating some aluminum (C(-A)-S-H), hydrotalcite-like phases, stratlingite, and amorphous geopolymer gel [13]. These systems suffer from significant autogenous and drying shrinkage and microcracking of the binder matrix. The final setting time can be very short; the strength development can be very fast. The durability, especially in acid exposures, is very good (Bernal et al., [14]). Fresh and hardened state properties of alkali-activated fly ash concrete strongly depend on the chemical composition of the precursor [15]. The reactivity of fly ash is relatively low leading to slow setting and the need for high curing temperatures [16]. Geopolymers based on metakaolin have usually slightly higher water demand and permeability in comparison with geopolymers based on fly ash or blast-furnace slag. The reaction product of metakaolin activated with sodium silicate and sodium hydroxide is usually an amorphous hydrated sodium aluminosilicate [17]. Some also reported formation of sodium alumina silicate hydrate gel (N-A-S-H) [18]. A relatively new approach uses

a combination of several types of aluminosilicates enabling to mitigate some of the pointed limitations. For example, the incorporation of slag into the fly ash-based system shortens the setting time, increases the compressive strength, and densifies the microstructure by formation of phases composed from modified calcium silicate hydrate gel (C-S-H). It includes aluminum modified calcium silicate hydrate (C-A-S-H) gel and sodium aluminosilicate hydrate (N-A-S-H) gel [19, 20]. Systems containing up to 75 wt.% of fly ash are formed by the coexistence of N-A-S-H and C-A-S-H. Systems with similar or lower fly ash to slag content form predominantly hybrid type of the N-(C)-A-S-H gel. It is believed that Ca released from slag is later incorporated into N-A-S-H gel formed from activation of fly ash. Slow dissolution of fly ash can be compensated with application of higher curing temperature, thus enabling formation of cross-linked products, densification of the microstructure, and increasing the strength of the solidified binder matrix [21]. The most commonly used alkali activators include sodium hydroxide, sodium silicate, sodium carbonate, and sodium sulphate [5]. Recently, effects of reactive magnesium oxide and calcium carbonate were also investigated; [22, 23]. The reactive magnesium oxide shortens the setting time and significantly reduces the drying shrinkage when used in blast furnace slag-based systems [24]. A small amount of crystalline phases combined with a higher magnesium oxide content tends to enhance the ultimate compressive strength [25]. The reactive magnesium oxide can be also used as a standalone alternative cementitious binder. The type of alkalis, the curing temperature, and the pH value of the solution affect the hydration of magnesium oxide into brucide [26–28]. The reactive magnesium oxide obtained from a light-burned periclase was studied, for example, by Zhang et al. [29]. Addition of silica fume resulted in formation of calcium silicate hydrate (C-S-H) gel and brucide. The brucide reacted with silica fume and formed magnesium silicate hydrate (M-S-H) gel. The obtained pH was below 10, which created a binder suitable for waste encapsulation.

The limestone is primarily used in Portland cement-based concretes as a filler to enhance the packing density. In the present study, the limestone was used in alkali-activated systems having very high pH of the pore solution. The very high alkalinity was assumed to be able to induce a limited chemical reactivity of limestone surface particles. The primary objective of this study was to determine the combined effects of reactive magnesia and calcium hydroxide on alkali-activated systems based on the mixture of limestone and metakaolin.

2. Materials and Methods

The experimental program was designed to determine basic mechanical properties, microstructure, and chemical composition of formed binder matrixes.

Magnesium oxide was supplied by Premier Magnesia, LLC; type Magox® Premium, metakaolin Argical-M 1200S by Imerys Minerals and limestone filler by Nordkalk-Finland. Their chemical compositions are shown in Table 1, and XRD spectra are shown in Figure 1. Three types of alkali activators were used: sodium hydroxide (NaOH), sodium silicate (Na_2SiO_3), and sodium sulphate (Na_2SO_4). Five mole solutions were prepared using deionized water and stored for 24 hours before mixing. The sodium hydroxide pellets were produced by Akzo Nobel and had NaOH content of 98.9%. The sodium silicate solution was supplied by PQ Finland Oy and had the molar ratio (SiO_2/Na_2O) of 2.00–2.10. Mix compositions are shown in Table 2. All mixes had an initial water to binder ratio of 0.6 adjusted during mixing to obtain a comparable workability. All mixes were produced using an Ecovac Bredent vacuum mixer with a capacity of 200 g. The vacuum mixer was used to remove entrapped air from the paste. The mixing time was 2 min, and the mixing speed was 290 rpm. All hardened samples had a dimension of $12 \times 1212 \times 60\,mm^3$ and were cast into Teflon moulds to exclude the effect of the demoulding oil. All specimens were demoulded after 24 hours and heat treated at 80°C for 24 hours. The compressive strength was determined after 3 and 28 days using the Zwick RK 250/50 loading machine, maintaining the loading rate of 0.35 mm/min. The identification of formed phases was done by X-ray diffraction (XRD) on 7-day old samples using a combination of Philips PW1710 diffractometer control unit, PW1820 goniometer, and a PW1830 generator with CuKα radiation. The generator voltage was 40 kV, and the current was 40 mA. The range of the 2θ angle was set at 5.015°–88.965° and the scan step at 0.03°. The thermogravimetric (TG) analysis was done using a DuPont Instruments 951 analyser, updated with a temperature programmer interface (TPI) controller. The heating rate was 20°C per minute, and the maximum temperature was 1000°C. Samples were heated in a helium atmosphere with a flow rate of 40 ml/min. The microstructure of hardened samples was determined using a field emission-scanning electron microscope- (FE-SEM)- type Quant FEG 450 produced by FEI. The used accelerating voltage was 5–10 keV, chamber pressure was 10–3 Pa, and a working distance was 15 mm. No additional conductive coating was applied to any of the specimens. The back-scattered electron (BSE) detector was used to obtain all images.

3. Test Results and Discussion

In general, the workability of all mixes tended to worsen when using sodium silicate and to a lesser extent with sodium hydroxide and sodium sulphate. Addition of magnesia to systems containing limestone and metakaolin worsened the workability while addition of calcium hydroxide had no effect. The observed worsening of the workability can be directly related to increased surface area and presumably, as not determined, lowering of the particle packing density [30]. In order to produce comparable mixes, the water-to-cement ratio was increased to compensate for the effect (Table 2).

Reference mixes containing only magnesia were used to determine effects of the alkali activator type on the hydration process. The sodium sulphate-activated mix had the highest 3- and 28-day compressive strength values reaching 22 MPa and 28 MPa, respectively, Figure 2. Pastes activated with

Table 1: Properties of metakaolin, limestone, and magnesia.

Material	Mean particle size (μm)	Specific surface area (m^2/g)	CaO + MgO	SiO_2	Al_2O_3	Fe_2O_3	$Na_2O + K_2O$	$CaCO_3$	LOI
Metakaolin	4.2	19	0.6	55	39	1.8	1	—	1
Limestone	10.7	—	49	9.2	1.9	0.87	0.61	71.3	42.8
Magnesia	5.0	110	99	0.35	0.1	0.15	—	—	4

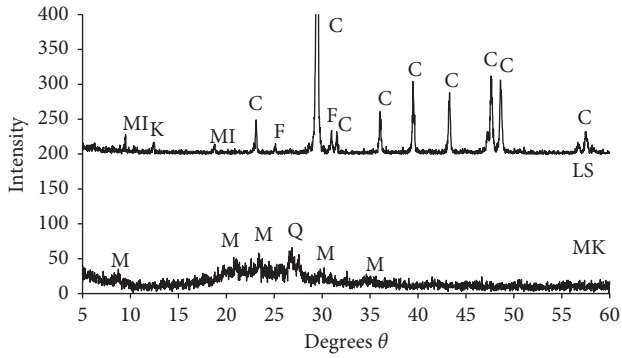

Figure 1: X-ray diffractgrams of metakaolin (MK) and limestone (LS). Phases marked are as follows: M: muscovite, Q: quartz, C: calcite, MI: mica, K: kaolinite, and F: feldspar.

Table 2: Mix composition.

Mix	MgO	MK	LS	Ca (O H)2	NaOH	NaSi	NaSO	Effective W/B ratio
MgOH	100	—	—	—	5	—	—	0.75
MgSi	100	—	—	—	—	5	—	0.85
MgSO	100	—	—	—	—	—	5	0.7
MOH3M	10	63	27	—	3	—	—	0.7
MOH3MC	10	56	24	10	3	—	—	0.7
MOH	—	45	45	10	5	—	—	0.65
MOHMgO	10	40	40	10	5	—	—	0.72
MSi	—	45	45	10	—	5	—	0.71
MSiMgO	10	40	40	10	—	5	—	0.79
MSO	—	45	45	10	—	—	5	0.62
MSOMgO	10	40	40	10	—	—	5	0.69

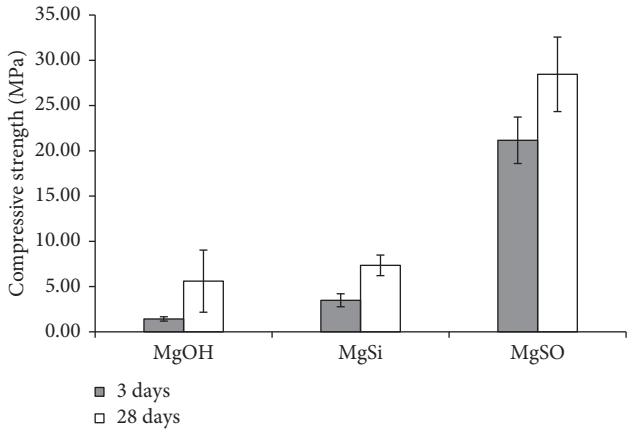

Figure 2: Effects of alkali activator type on the strength development of magnesia pastes.

sodium hydroxide reached only 2 and 5 MPa after 3 and 28 days while sodium sulphate-activated pastes reached 4 and 8 MPa. The recorded variations in compressive strength values are related to both water-to-binder ratio and to chemical processes controlled by the used alkali activator. However, no direct correlation between the water-to-binder ratio and the strength was observed, thus indicating that the type of the activator had a dominative role in ongoing dissolution and hydration processes. Hardened matrixes were composed of magnesium hydroxide (B), also observed by Skorb et al. [31] (Figure 3). Unreacted magnesia (M) was detected only in mixes activated with sodium silicate and sodium hydroxide. The TG analysis revealed peaks, at 100°C, between 350 and 400°C, and at 600°C (Figure 4). The first peak can be directly related to the moisture evaporation while the second to the decomposition of magnesium hydroxide [26]. The third decomposition peak located at around 600°C is related to magnesium carbonate $MgCO_3$ [32].

Reference mixes MOH3M and MOH3MCa were used to verify effects of calcium hydroxide on limestone-metakaolin-magnesia alkali-activated systems. Replacement of the binder by 10 wt.% of calcium hydroxide increased the 28-day compressive strength by 400%, Figure 5, presumably due to formation of a N-A-S-H gel [33] and Granzio et al. [18].

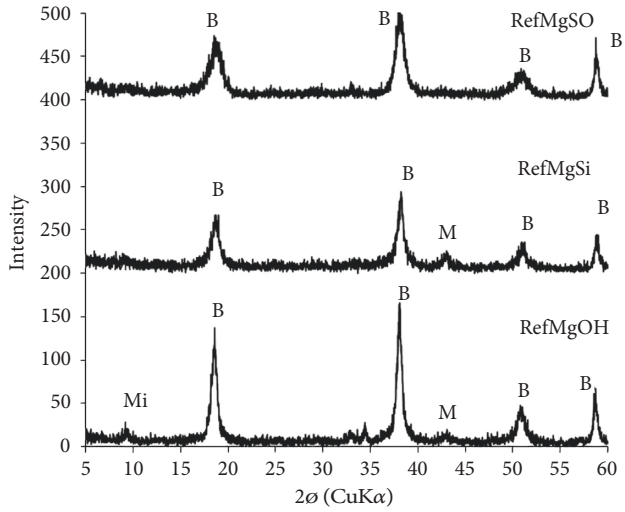

Figure 3: XRD spectra of magnesia mixes alkali activated with sodium hydroxide, sodium silicate, and sodium sulphate. B: brucide, M: magnesia, and Mi: mika.

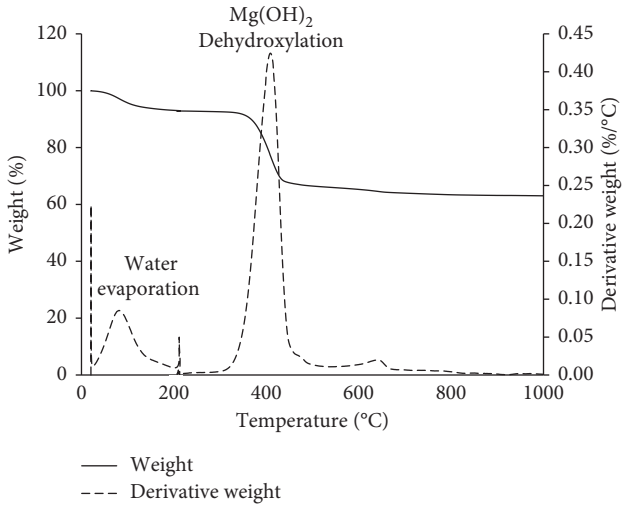

Figure 4: TG and DTG of magnesia paste activated with $NaSO_3$.

Others observed formation of sodium aluminosilicate and secondary CSH gel [34]. Curing temperature, concentration of alkalis, solid content, and the type of alkalis affected formation of these phases. The metakaolin-to-calcium hydroxide ratio did not influence the rate of aluminosilicate formation but promoted precipitation of larger reaction products when this ratio was increasing. Higher additions of calcium hydroxide appeared to produce mixes with better mechanical properties especially when using heat curing [34]. In the present study, all metakaolin-limestone mixes contained 10 wt.% of calcium hydroxide and optionally 10 wt.% of magnesia. The 3-day compressive strength increased for all magnesia containing mixes depending on the type of the used activator, (Figure 6). The highest increase from 7 MPa to 12 MPa was measured for sodium sulphate-activated mix MSOMgO and the lowest increase by only 0.5 MPa for sodium silicate-activated mix

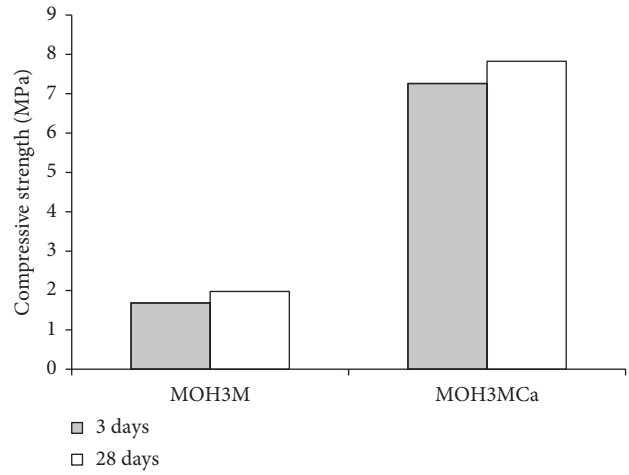

Figure 5: Effects of calcium hydroxide on strength development of limestone/metakaolin system activated with sodium hydroxide.

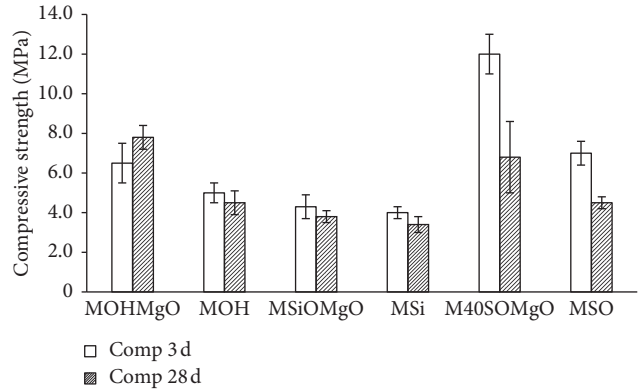

Figure 6: Effects of magnesia on strength development of limestone/metakaolin/calcium hydroxide systems.

MSiOMgO. On the contrary, the 28-day compressive strength showed regression in nearly all studied mixes. The effect was especially pronounced for mixes containing magnesia and activated with sodium sulphate. In this case, the strength decreased by nearly 50%. The observed regression could be related to the initial formation of an unstable geopolymer gel followed by its later collapse [9, 35]. However, a consequence of a lower tensile strength combined with a presumably higher shrinkage resulted in microcracking of the hardened binder matrix (Figure 7). On the contrary, magnesia prevented strength regression of the mix activated with sodium hydroxide. It could be related to the formation of more stable crystalline phases intermixed with brucide instead of the unstable gel (Figure 8(a)).

The combined effect of the reactive magnesia and calcium hydroxide was an increased compressive strength and a lack of the strength regression. The effect was only present in limestone-metakaolin mixes activated with the sodium hydroxide.

The X-ray diffractgrams of 28-day old pastes showed a generally high amount of the unreacted calcium carbonate (C) with smaller amounts in the case of pastes activated with

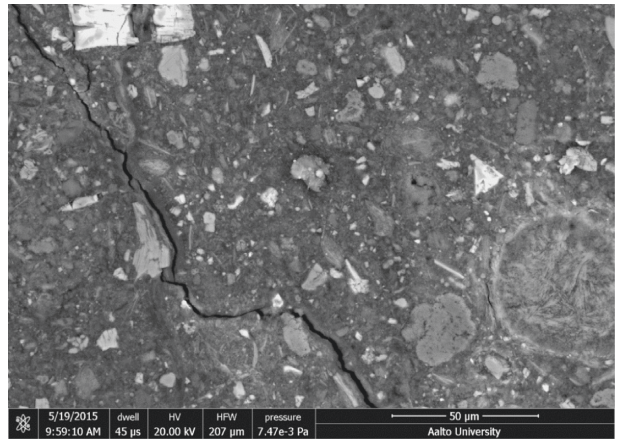

Figure 7: BSE-SEM images of 28-day old mix MSOMgO

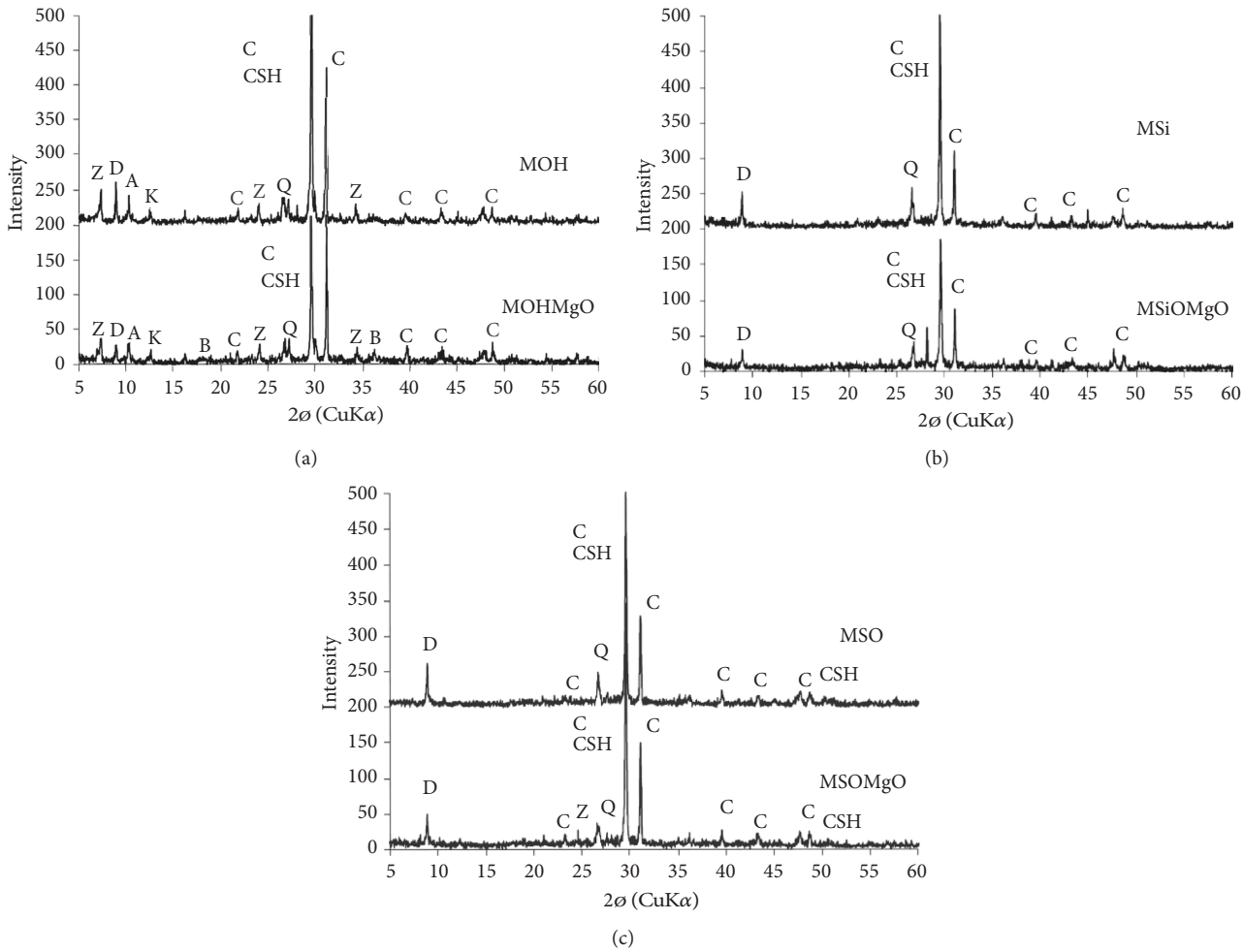

Figure 8: XRD spectra of 28-day old limestone/metakaolin/calcium hydroxide with and without magnesia. C: calcite, Z: zeolite, A: AFM phase, D: additional layered calcium carboaluminate phase, M: muscovite, MI: mica, Q: quartz, and K: kaolinite.

sodium hydroxide and sodium silicate. This indicates a higher dissolution rate of limestone of those mixes (Figure 8) [22]. Layered calcium carboaluminate (D) phase was identified to form in all mixes but with a lower amount forming in the presence of magnesia.

Brucide peaks (B) were detected only in the mix MOHMgO containing magnesia and activated with sodium hydroxide (Figure 8(a)). A lack of brucide formation in the presence of magnesia was also observed earlier for the blast-furnace slag-based binders. The hydrolysis of MgO on the

surface of BFS and the reaction with broken Si-0 or Al-0 bonds forming magnesium silicate hydrate (M-S-H) was indicated as the main cause. The formation of M-S-H could in turn hinder precipitation of brucide. The detection of M-S-H in XRD is difficult what could explain its absence in XRD spectra shown in Figure 8 [36, 37]. Peaks marked as "CSH" and detected at around 29° θ were identified as originating from a mix of poorly crystalline sodium- and aluminum- substituted calcium silicate hydrate C-(N)-A-S-H based on the earlier study by Walkley at al. [38]. In that study, high purity synthetic calcium aluminosilicate powder was used as a precursor. The increased Ca content in the precursor, in the present study, addition of Ca $(OH)_2$, resulted presumably in a predominant formation of a low Al, high Ca C-(N)-A-S-H. Partial overlap of this peak with calcite made comparison between mixes difficult; however, the amount of formed phases depends on the type of the used alkali activator. Consequently, formation of C-(N)-A-S-H gel could be retarded due to the presence of sulphate ions in the pore solution which could repel the negative charge on the aluminosilicates. This would in turn obstruct condensation reactions and would lower the degree of ash solubilization due to the slight decline of pH [37]. Sulphate could also accelerate the conversion of Ca-(N)-A-S-H gel into zeolites, Abdel-Gawwad [37], which was confirmed by detection of zeolite-like "Z" peaks in the XRD analysis. Existence of nanometer-sized crystalline zeolite structures in generally XRD-amorphous geopolymer gels has been suggested by others [39]. A typical effect related to the presence of zeolites in geopolymer gels is an improvement of mechanical properties which could be also observed in all mixes, where the zeolite-related peak was detected. A lack of zeolites in mixes activated with sodium silicate can be directly linked to a formation of templates for an assembly of aluminates by variety of silicate units originating for that activator [40]. Consequently, the formation of zeolites is suppressed, and instead, amorphous products are formed due to a slow condensation between Al-OH from metakaolin and Si-OH from sodium silicate. It is unclear why the zeolite did not form in the mix activated by sodium sulphate not containing magnesia.

The SEM micrograph (Figures 7, 9, and 10) clearly shows the least porous microstructure in mixes activated with sodium hydroxide which combined with a higher crystallinity detected in XRD that indicates less dense amorphous gel which complies with earlier results; [40]. On the contrary, mixes activated with sodium silicate and sodium sulphate showed less crystallinity in XRD and also dense microstructure in SEM. The presence of magnesia visibly densified the binder matrix especially in the case of the mix activated with sodium hydroxide (Figure 9). It could be related to the presence of magnesium silicate hydrate, which hindered the formation of brucide. The binder matrix of the mix activated with sodium sulphate showed the highest 3-day compressive strength, and subsequent strength regression after 28 days appeared to be severely cracked (Figure 7). Cracking can be linked to shrinkage of the unstable geopolymer gel.

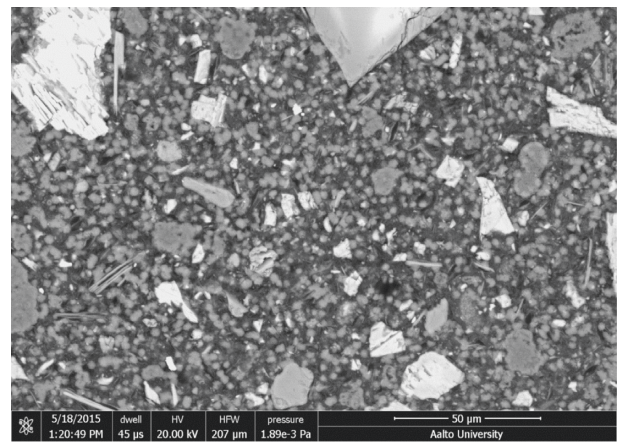

(a)

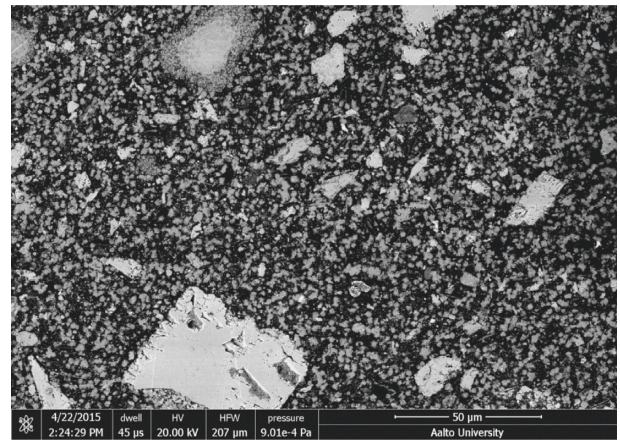

(b)

Figure 9: BSE-SEM images of 28-day old mixes: (a) MOHMgO and (b) MOH.

4. Conclusions

Alkali activation of a reactive magnesium oxide produced matrixes with compressive strengths of up to 28 MPa when activated with sodium sulphate. Alkali activators worsened the workability of fresh mixes with sodium silicate having the strongest effect and sodium sulphate the weakest. The presence of calcium hydroxide increased the compressive strength of hardened matrixes by 400%. Magnesia increased the early-age strength of metakaolin-limestone systems by up to 90% when activated with sodium sulphate but caused its later regression by 50% in the case of this activator. Mixes with other activators showed increase of the compressive strength by just few present and also later regression. Formation of an unstable gel followed by its collapse leading to a low tensile strength, higher shrinkage, and eventually to microcracking of the binder matrix could be a possible mechanism behind the observed regression. The trend was not observed in the mix activated with sodium hydroxide and containing magnesia. In that case, more stable crystalline phases intermixed with brucide were formed. Magnesia densified the binder matrix by increasing the amount of amorphous phases on the expense of less crystalline phases. Furthermore, sodium silicate hindered formation of

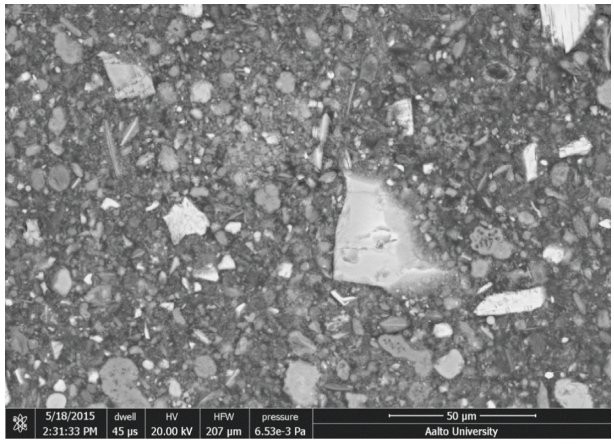

(a)

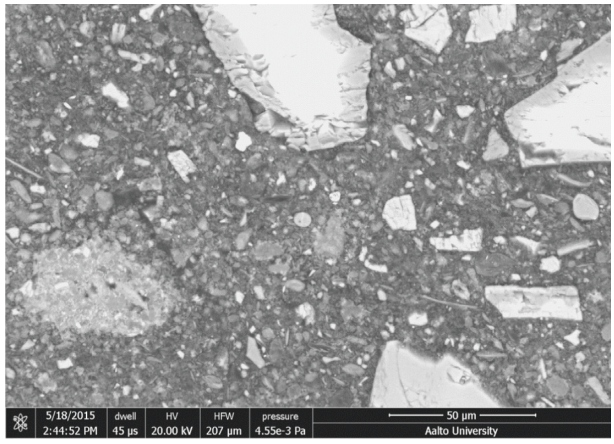

(b)

Figure 10: BSE-SEM images of 28-day old mixes: (a) MSiMgO and (b) MSi.

C-(N)-A-S-H gel. Combination of reactive magnesia and calcium hydroxide increased the compressive strength and prevented its regression at the later age. Unfortunately, the recorded ultimate strength of this system was lower in comparison with systems activated with sodium sulphate but which also showed the highest regression. The possible causes of the observed regression should be further studied.

Data Availability

The data used to support the findings of this study are available from the corresponding author upon request.

Conflicts of Interest

The authors declare that they have no conflicts of interest.

References

[1] R. M. Andrew, "Global CO2 emissions from cement production," *Earth System Science Data*, vol. 10, no. 1, pp. 195–217, 2018.

[2] J. L. Provis, "Alkali-activated materials," *Cement and Concrete Research*, 2017.

[3] A. O. Purdon, "The action of alkalis on blast-furnace slag," *Journal of the Society of Chemical Industry*, vol. 59, pp. 191–202, 1940.

[4] J. L. Provis and J. S. van Deventer, *Alkali Activated Materials: State-of-the-art Report, RILEM TC 224-AAM*, Springer, Dordrecht, Netherlands, 2014, ISSN 978-94-007-7672-2.

[5] C. Shi, P. V. Krivenko, and D. M. Roy, *Alkali-Activated Cements and Concretes*, Taylor & Francis, Abingdon, UK, 2006.

[6] T. B. Husbands, P. G. Malone, and L. D. Wakeley, *Performance of Concretes Proportioned with Pyrame Blended Cement, Vicksburg, MS, USA*, 1994.

[7] J. L. Provis and J. S. J. van Deventer, "Geopolymerisation kinetics. 1. In situ energy- dispersive X-ray diffractometry," *Chemical Engineering Science*, vol. 62, no. 9, pp. 2309–2317, 2007.

[8] J. L. Provis and J. S. J. van Deventer, *Geopolymers: Structure, Processing, Properties and Industrial Applications*, Woodhead, Cambridge, UK, 2009.

[9] A. Cwirzen, R. Engblom, J. Punkki, and K. Habermehl-Cwirzen, "Effects of curing: comparison of optimized alkali-activated PC-FA-BFS and PC concretes," *Magazine of Concrete Research*, vol. 66, no. 6, pp. 315–323, 2014.

[10] A. Humad, L. J. Provis, and A. Cwirzen, "Alkali activation of a high MgO GGBS—fresh and hardened properties," *Magazin of Concrete Research*, 2017.

[11] C. E. White, J. L. Provis, T. Proffen, D. P. Riley, and J. S. J. van Deventer, "Density functional modeling of the local structure of kaolinite subjected to thermal dihydroxylation," *Journal of Physical Chemistry A*, vol. 114, pp. 4988–4996, 2010.

[12] C. E. White, J. L. Provis, T. Proffen, D. P. Riley, and J. S. J. van Deventer, "Combining density functional theory (DFT) and pair distribution function (PDF) analysis to solve the structure of metastable materials: the case of metakaolin," *Physical Chemistry Chemical Physics*, vol. 12, no. 13, pp. 3239–3245, 2010.

[13] B. Lothenbach and A. Gruskovnjak, "Hydration of alkali-activated slag: thermodynamicmodeling," *Advances in Cement Research*, vol. 19, pp. 81–92, 2007.

[14] S. A. Bernal and J. L. Provis, "Durability of alkali-activated materials: progress and perspectives," *Journal of the American Ceramic Society*, vol. 97, no. 4, pp. 997–1008, 2014.

[15] A. Motorwala, V. Shah, R. Kammula, P. Nannapaneni, and D. B. Raijiwala, "Alkali Activated fly ash based geopolymer concrete," *International Journal of Emerging Technology and Advanced Engineering*, vol. 3, no. 1, pp. 159–166, 2013.

[16] H. Bakkali, M. Ammari, and I. Frar, "NaOH alkali-activated class F fly ash: NaOH molarity, Curing conditions and mass ratio effect," *Journal of Materials and Environmental Science*, vol. 7, no. 2, pp. 397–401, 2016.

[17] M. L. Granizo, M. T. Branco Varela, and S. Martinez-Ramirez, "Alkali activation of metakaolins: parameters affecting mechanical, structural and microstructural properties," *Journal of Materials Science*, vol. 42, no. 9, pp. 2934–2943, 2007.

[18] M. L. Granizo, S. Alonso, M. T. Blanco-Varela, and A. Palomo, "Alkaline activation of metakaolin: effect of calcium hydroxide in the products of reaction," *Journal of American Ceramic Society*, vol. 85, no. 1, pp. 225–231, 2002.

[19] S. A. Bernal, J. L. Provis, B. Walkley, R. San Nicolas, J. D. Gehman, and D. G. Brice, "Gel nanostructure in alkali-activated binders based on slag and fly ash, and effects of accelerated carbonation," *Cement and Concrete Research*, vol. 53, pp. 127–144, 2013.

[20] I. Garda-Lodeiro, A. Palomo, A. Fernandez-Jimenez, and D. E. Macphee, "Compatibility studies between N-A-S-H and

C-A-S-H gels. Study in the ternary diagram Na_20-CaO-$A_2'0$rSiOrH_20," *Cement and Concrete Research*, vol. 41, no. 9, pp. 923–931, 2011.

[21] I. Ismail, S. A. Bernal, J. L. Provis, R. San Nicolas, S. Hamdan, and J. S. J. van Deventer, "Modification of phase evolution in alkali-activated blast furnace slag by the incorporation of fly ash," *Cement and Concrete Composites*, vol. 45, no. 1, pp. 125–135, 2014.

[22] F. Jin, K. Gu, and A. Al-Tabbaa, "Strength and drying shrinkage of reactive MgO modified alkali-activated slag paste," *Construction and Building Materials*, vol. 51, pp. 395–404, 2014.

[23] A. Cwirzen, J. L. Provis, V. Penttala, and K. Habermehl-Cwirzen, "The effect of limestone on sodium hydroxide-activated metakaolin-based geopolymers," *Construction and Building Materials*, vol. 66, pp. 53–62, 2014.

[24] D. Feng, J. L. Provis, and J. S. J. van Deventer, "Thermal activation of albite for the synthesis of one-part mix geopolymers," *Journal of the American Ceramic Society*, vol. 95, no. 2, pp. 565–572, 2012.

[25] E. Demoulian, P. Gourdin, F. Hawthorn, and C. Vernet, "Influence of slags chemical composition and texture on their hydraulicity," in *Proceedings of 7th International Conference on Cement Chemistry*, Paris, France, 1980.

[26] M. Maryska and J. Blaha, "Hydration kinetics of magnesium oxide, Part 3–hydrationrate of MgO in terms of temperature and time of its firing," *Ceramics-Silikaty*, vol. 41, no. 4, pp. 121–123, 1997.

[27] K. P. Matabola, E. M. van der Merwe, C. A. Strydom, and F. J. W. Labuschagned, "The influence of hydrating agents on the hydration of industrial magnesium oxide," *Journal of Chemical Technology and Biotechnology*, vol. 85, no. 12, pp. 1569–1574, 2010.

[28] D. Filippou, N. Katiforis, N. Papassiopi, and K. Adam, "On the kinetics of magnesia hydration in magnesium acetate solutions," *Journal of Chemical Technology*, vol. 74, no. 4, pp. 322–328, 1999.

[29] T. Zhang, L. J. Vandeperre, and C. R. Cheeseman, "Formation of magnesium silicate hydrate (M-S-H) cement pastes using sodium hexametaphosphate," *Cem Conc Res*, vol. 65, pp. 8–14, 2014.

[30] A. Cwirzen, V. Penttala, and C. Vornanen, "Reactive powder based concretes: mechanical properties, durability and hybrid use with OPC," *Cement and Concrete Research*, vol. 38, no. 10, pp. 1217–1226, 2008.

[31] E. V. Skorb, D. Fix, D. G. Shchukin et al., "Sonochemical formation of metal sponges," *Nanoscale*, vol. 3, pp. 985–993, 2011.

[32] J. J. Thomas, S. Musso, and I. Prestini, "Kinetics and activation energy of magnesium oxide hydration," *Journal of the American Ceramic Society*, vol. 97, no. 1, pp. 275–282, 2014.

[33] X. Guo and H. Shi, "Metakaolin-, fly ash- and calcium hydroxide-based geopolymers: effects of calcium on performance," *Advances in Cement Research*, vol. 27, no. 10, pp. 559–566, 2015.

[34] S. Alonso and A. Palomo, "Alkaline activation of metakaolin and calcium hydroxide mixtures influence of temperature, activator concentration and solids ratio," *Materials Letters*, vol. 47, no. 1-2, pp. 55–62, 2001.

[35] R. R. Lloyd, "Accelerated ageing of geopolymers," in *Geopolymers: Structure, Processing, Properties and Industrial Applications*, J. L. Provis and J. S. J. van Deventer, Eds., pp. 139–166, Woodhead, Cambridge, UK, 2009.

[36] D. R. M. Brew and F. P. Glasser, "Synthesis and characterization of magnesium silicate hydrate gels," *Cement and Concrete Research*, vol. 35, no. 1, pp. 85–98, 2005.

[37] H. A. Abdel-Gawwad, "Effect of reactive magnesium oxide on properties of alkali- activated slag-cement pastes," *Journal of Materials in Civil Engineering*, vol. 27, no. 8, 2014.

[38] B. Walkley, R. San Nicolas, M. A. Sani et al., "Phase evolution of C-(N)-A-S-H/N-A-S-H gel blends investigated via alkali-activation of synthetic calcium aluminosilicate precursors," *Cement and Concrete Research*, vol. 89, pp. 120–135, 2016.

[39] J. L. Provis, G. C. Lukey, and J. S. J. van Deventer, "Do geopolymers actually contain nanocrystalline zeolites? A Re-examination of existing results," *Chemistry of Materials*, vol. 17, no. 12, pp. 3075–3085, 2005.

[40] B. Zhang, K. J. D. Mackenzie, and I. W. M. Brown, "Crystalline phase formation in metakaolinite geopolymers activated with NaOH and sodium silicate," *Journal of Material Science*, vol. 44, no. 17, pp. 4668–4676, 2009.